

# Quadrivariate Empirical Mode Decomposition

Naveed ur Rehman, *Student Member, IEEE* and Danilo P. Mandic, *Senior Member, IEEE*

**Abstract**—We introduce a quadrivariate extension of Empirical Mode Decomposition (EMD) algorithm, termed QEMD, as a tool for the time-frequency analysis of nonlinear and non-stationary signals consisting of up to four channels. The local mean estimation of the quadrivariate signal is based on taking real-valued projections of the input in different directions in a multidimensional space where the signal resides. To this end, the set of direction vectors is generated on 3-sphere (residing in 4D space) via the low-discrepancy Hammersley sequence. It has also been shown that the resulting set of vectors is more uniformly distributed on a 3-sphere as compared to that generated by a uniform angular coordinate system. The ability of QEMD to extract common modes within multichannel data is demonstrated by simulations on both synthetic and real-world signals.

**Index Terms**—Quadrivariate signal analysis, Empirical mode decomposition (EMD), Intrinsic mode functions (IMFs), multi-scale analysis, EEG artifact separation, RGB image decomposition.

## I. INTRODUCTION

The empirical mode decomposition (EMD) algorithm has become an established tool for the decomposition and time-frequency analysis of nonlinear and non-stationary signals [1]. Using EMD, the original signal is decomposed as a linear combination of intrinsic oscillatory modes, called Intrinsic Mode Functions (IMFs). The IMFs are defined in such a way that the subsequent application of Hilbert transform provides meaningful instantaneous frequency estimates [2]. Due to the fully data driven nature of EMD, it has found numerous applications in the analysis of real world nonlinear and non-stationary signals [3] [4].

The recent advances in engineering and biomedicine have given rise to new issues related to complexity, nonlinearity and multichannel dynamics in real world systems. These problems can be tackled more effectively if the resulting multichannel dataset is processed directly in the domain where it resides, that is, via algorithms designed specifically for multivariate signals.

The need to develop EMD extensions is further accentuated by the fact that recent multivariate extensions of EMD, including those for the processing of bivariate [5] [6] [7] and trivariate [8] signals, have shown considerable potential in information extraction, owing to their ability to extract common modes within the multivariate IMFs representing multichannel data [9]. This cannot be achieved by applying the standard univariate EMD algorithm to each channel separately. The bivariate and trivariate extensions of EMD

have, therefore, found applications in e.g. synchrony analysis of multichannel EEG signals and image fusion [9]. An extension of EMD capable of simultaneously processing any number of channels has also been recently proposed [10]. In this work, we aim to shed more light on the methodology suitable for the quadrivariate (quaternion) signals, and especially on the synchronization of information spread across multiple channels, which in turn paves the way for its use in data synchronization and fusion applications.

An important step in multivariate extensions of EMD is the computation of the local mean of the signal. All existing methods employ multiple real-valued projections of the input signal in several directions, in their respective multidimensional spaces, to calculate the local mean [6] [8]. To generate the direction vector in multidimensional spaces, the bivariate and trivariate EMD use uniform angular sampling; while the same idea can be used for a general class of n-variate signals using the uniform angular (hyperspherical coordinate) system, the multivariate EMD [10] employs a much improved low-discrepancy Hammersley based sampling to generate the direction vectors. In this paper, we consider the specific case of quadrivariate signals to show the superiority of the Hammersley based sampling method over the uniform angular sampling techniques.

The paper is organized as follows: bivariate and trivariate extensions of EMD are discussed in Section 2. Section 3 introduces the proposed quadrivariate EMD method, Section 4 illustrates the mode alignment property of the proposed method on a synthetic quaternion signal. The potential of the proposed method (QEMD) in information extraction from noisy EEG signals and image decomposition has also been illustrated.

## II. EXISTING MULTIVARIATE EXTENSIONS OF EMPIRICAL MODE DECOMPOSITION

The standard Empirical Mode Decomposition (EMD) method decomposes the original signal into a finite set of oscillatory components, termed Intrinsic Mode Functions (IMFs). More specifically, for a real valued signal  $x(k)$ , the standard EMD finds a set of  $N$  IMFs  $\{c_i(k)\}_{i=1}^N$ , and a monotonic residue signal  $r(k)$ , so that

$$x(k) = \sum_{i=1}^N c_i(k) + r(k) \quad (1)$$

To ensure well behaved time frequency spectra, IMFs  $c_i(k)$  are defined so as to have symmetric upper and lower envelopes, with the number of zero crossings and the number of extrema differing at most by one. An iterative process called the sifting algorithm is employed to extract IMFs; for

N. Rehman and D. P. Mandic are associated with the Communications and Signal Processing group within the department of Electrical and Electronic Engineering, Imperial College London, London, UK, SW7 2AZ. (phone: +44 (0) 207-594-6271; email: naveed.rehman07, d.mandic@imperial.ac.uk).

illustration, a sifting procedure for obtaining the first IMF from the signal  $x'(k)$  is outlined in Algorithm 1.

---

**Algorithm 1** The standard EMD algorithm

---

- 1: Find the locations of all the extrema of  $x'(k)$ ;
  - 2: Interpolate (using cubic spline interpolation) between all the minima (resp. maxima) to obtain the lower signal envelope,  $e_{min}(k)$  (resp.  $e_{max}(k)$ );
  - 3: Compute the local mean  $m(k) = [e_{min}(k) + e_{max}(k)]/2$ ;
  - 4: Subtract the mean from the signal to obtain the ‘‘oscillatory mode’’  $s(k) = x'(k) - m(k)$ ;
  - 5: If  $s(k)$  obeys the stopping criteria,  $d(k) = s(k)$  becomes an IMF, otherwise set  $x'(k) = s(k)$  and repeat the process from Step 1.
- 

Once the first IMF is obtained, the same procedure is applied iteratively to the residual  $r(k) = x(k) - d(k)$  to extract the remaining IMFs. The standard stopping criterion terminates the sifting process only after the above condition for an IMF is met for  $S$  consecutive times [11].

*A. Bivariate/Complex extensions of EMD*

The first complex extension of EMD [5] employed the concept of analytical signal and subsequently applied standard EMD to analyse complex/bivariate data; however, this method cannot guarantee equal number of real and imaginary IMFs, thus limiting its applications. An extension of EMD which operates fully in the complex domain was first proposed in [7], termed rotation-invariant EMD (RI-EMD). The extrema of a complex/ bivariate signal are chosen to be the points where the angle of the derivative of the complex signal becomes zero, that is, based on the change in the phase of the signal. The signal envelopes are produced by using component-wise spline interpolation, and the local maxima and minima are then averaged to obtain the local mean of the bivariate signal.

The RI-EMD algorithm uses effectively only the extrema of the imaginary part of the complex signal, which results in envelopes based on only two projected directions. An algorithm which gives more accurate values of the local mean is the Bivariate EMD (BEMD) [6], where the envelopes corresponding to multiple directions in the complex plane are generated, and then averaged to obtain the local mean. The set of direction vectors for projections are chosen as equidistant points along the unit circle. The zero mean rotating components, embedded in the input bivariate signal then become bivariate/complex-valued IMFs. The RI-EMD and BEMD algorithms are equivalent for  $K = 4$  direction vectors.

*B. Trivariate EMD*

An extension of EMD to trivariate signals has been recently proposed in which the estimation of the local mean and envelopes of a trivariate signal is performed by taking projections along multiple directions in three dimensional (3D) spaces [8]. To generate a set of multiple direction vectors in a 3D space, a lattice is created by taking equidistant

points on multiple longitudinal lines on the sphere (obtaining so called ‘‘equi-longitudinal lines’’). The 3D rotating components are thus embedded within the input signal as pure quaternion IMFs.

III. THE PROPOSED QUADRIVARIATE EMD ALGORITHM

In real-valued EMD, the local mean is computed by taking an average of upper and lower envelopes, which in turn, are obtained by interpolating between the local maxima and minima. However, in general, for multivariate signals the concept of local maxima and minima is difficult to interpret. Moreover, the notion of ‘oscillatory modes’ defining an IMF is rather confusing for multivariate signals. This has led to an idea of estimating the local mean of bivariate and trivariate signals by taking an average of their multiple real-valued projections along different directions [6] [8].

Similarly for quadrivariate signals, the local mean can be estimated by taking projections along different directions in 4D spaces. The maxima of the projected signals are interpolated to yield multiple signal envelopes, which are then averaged to obtain the local mean of the quadrivariate signal. The idea of mapping an input quadrivariate signal onto multiple real valued ‘projected’ signals, to generate multidimensional envelopes, can therefore be seen as a generalisation of the concept employed in the existing bivariate [6] and trivariate [8] extensions of EMD. The resulting quaternion valued IMFs represent rotational modes embedded within quadrivariate data.

An important issue in this regard is the selection of direction vectors in 4D spaces, a necessary step for taking signal projections. These vectors must be chosen so as to be uniformly distributed in order to reduce the computational time and increase the accuracy of the algorithm. Since the direction vectors in 4D spaces can be equivalently represented as points on a 3-sphere (which resides in a 4D space), therefore, the problem of finding a suitable set of direction vectors can be treated as that of choosing a suitable sampling method on a 3-sphere.

*A. Uniform angular sampling*

As an extension of sampling in bivariate and trivariate EMD, a simple choice for finding the direction vectors in 4D space would be to perform uniform angular sampling of a 3-sphere, using the so called hyperspherical coordinate system. To generate a pointset for a general case of an  $(n-1)$ -sphere, consider the  $n$ -sphere with centre point  $C$  and radius  $R$ , given by

$$R = \sum_{j=1}^{n+1} (x_j - C_j)^2. \quad (2)$$

A coordinate system in an  $n$ -dimensional Euclidean space can then be defined to serve as a pointset (and the corresponding set of direction vectors) on an  $(n-1)$ -sphere. Let  $\{\theta_1, \theta_2, \dots, \theta_{(n-1)}\}$  be the  $(n-1)$  angular coordinates, then

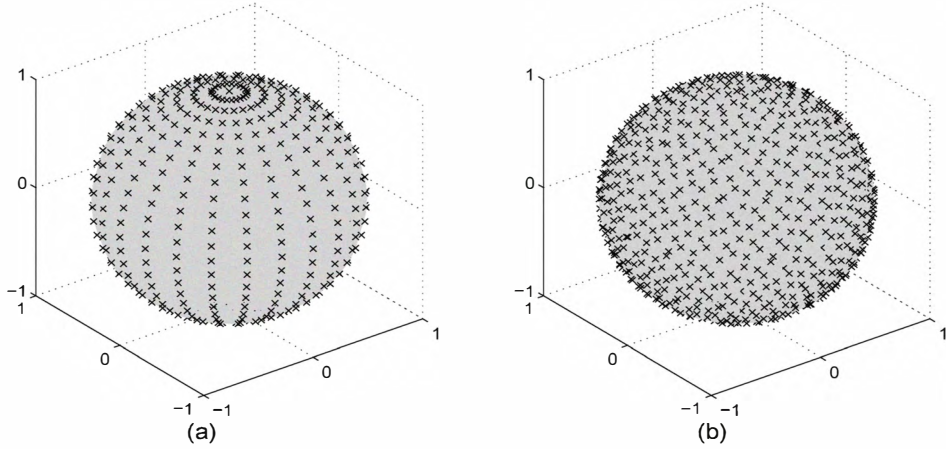


Fig. 1. Direction vectors for taking projections of trivariate signals on a 2-sphere generated by using (a) spherical coordinate system; (b) a low-discrepancy Hammersley sequence.

an  $n$ -dimensional coordinate system having  $\{x_i\}_{i=1}^n$  as the  $n$  coordinates on a unit  $(n-1)$ -sphere is given by:

$$\begin{aligned}
 x_1 &= \cos \theta_1 \\
 x_2 &= \sin \theta_1 \times \cos \theta_2 \\
 x_3 &= \sin \theta_1 \times \sin \theta_2 \times \cos \theta_3 \\
 &\vdots \\
 x_{n-1} &= \sin \theta_1 \times \cdots \times \sin \theta_{n-2} \times \cos \theta_{n-1} \\
 x_n &= \sin \theta_1 \times \cdots \times \sin \theta_{n-2} \times \sin \theta_{n-1}. \quad (3)
 \end{aligned}$$

For a special case of  $n = 4$ , (3) can be used to generate a set of direction vectors on a 3-sphere for taking projections of a quadrivariate signal. Note that for  $n = 2$  and  $n = 3$ , (3) corresponds, respectively, to the samples generated from polar and spherical coordinate systems.

### B. Sampling based on Hammersley sequence

While the uniform angular sampling method provides satisfactory solution in the case of bivariate and trivariate signals, it produces largely non-uniformly distributed sample sets for higher dimensional signals. Even for trivariate signals, it generates the point set having greater concentration at poles of the sphere as compared to the equator (see Figure 1(a)). This effect is expected to be even more pronounced in the case of quadrivariate signals. To tackle this problem, we propose the sampling scheme to generate the point set (direction vectors) in 4D spaces via the low-discrepancy Hammersley sequence. This yields improved generalized discrepancy estimates as compared to other sampling methods (including uniform angular sampling), and hence, provides more uniformly distributed sampling on a sphere [12]. This, in turn, gives a suitable set of direction vectors for generating signal projections and the corresponding signal envelopes, ensuring enhanced local mean estimates.

To generate the Hammersley sequence, let  $x_1, x_2, \dots, x_n$  be the first  $n$  prime numbers; then the  $i$ th sample of a one

dimensional Halton sequence, denoted by  $r_i^x$ , is given by

$$r_i^x = \frac{a_0}{x} + \frac{a_1}{x^2} + \frac{a_2}{x^3} + \cdots + \frac{a_s}{x^{s+1}} \quad (4)$$

where the base- $x$  representation of  $i$  is given by

$$i = a_0 + a_1 \times x + a_2 \times x^2 + \cdots + a_s \times x^s \quad (5)$$

Starting from  $i = 0$ , the  $i$ th sample of the Halton sequence then becomes

$$(r_i^{x_1}, r_i^{x_2}, \dots, r_i^{x_n}) \quad (6)$$

The Hammersley sequence is used when the total number of samples  $N$  is known apriori; in this case, the  $i$ th sample within the Hammersley sequence is calculated as

$$(i/N, r_i^{x_1}, r_i^{x_2}, \dots, r_i^{x_{n-1}}) \quad (7)$$

For quadrivariate signals,  $n = 4$  is used, and for trivariate signals,  $n = 3$ . For illustration, Figure 1(b) and Figure 2 show, respectively, the pointsets on the surface of the sphere (2-sphere) and hypersphere (3-sphere), generated by the low discrepancy Hammersley sequence. Observe that, as desired, the points generated in this way are more uniformly distributed. In Figure 2, ideally, the pointset should be plotted on a 3-sphere, however, for visualisation purposes, we can only use three 2-spheres.

Consider an input quaternion signal  $q$ , and let  $\mathbf{x}^{\theta^k} = \{x_1^k, x_2^k, x_3^k, x_4^k\}$  denote a set of direction vectors along the directions given by angles  $\theta^k = \{\theta_1^k, \theta_2^k, \theta_3^k\}$  on a hypersphere (3-sphere). Then the proposed quaternion extension of EMD suitable for operating on general nonlinear and nonstationary quaternion time series is summarised in Algorithm 2.

### C. The Stopping Criteria for quadrivariate EMD

The standard stopping criteria in EMD requires IMFs to be designed in such a way that the number of extrema and the zero crossings differ at most by one for  $S$  consecutive

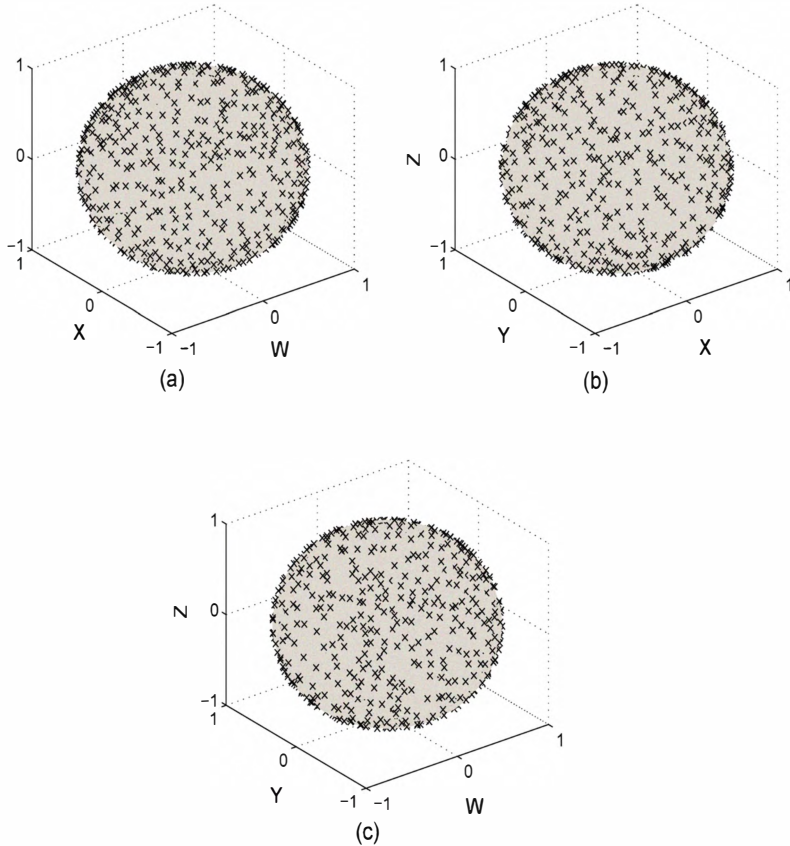


Fig. 2. Direction vectors for taking projections of a quaternion signal (with  $N=4$  components) on a unit 3-sphere generated by using a low discrepancy Hammersley sequence. For visualisation purposes, the pointset is plotted on three unit 2-spheres, defined respectively by the  $WXY$ ,  $XYZ$ , and  $WYZ$  axes.

iterations of the sifting algorithm. The optimal empirical value of  $S$  has been observed to be in the range of 2–3 [11].

Similarly, in [13], an improved stopping criterion is presented, which introduces an evaluation function based on the envelope amplitude, defined as  $a(t) = e_{max}(t) - e_{min}(t)$ , so that the sifting process is continued till the value of the evaluation function, which is defined as  $f(t) = |\frac{m(t)}{a(t)}|$ , where  $m(t)$  is the local mean signal, is greater or equal to some predefined thresholds. In the multivariate EMD algorithm, we can apply both the above criteria to all projections of the input signal and stop the sifting process once the stopping condition is met for all projections. Another possible method may be to stop the sifting process once the stopping criteria is met for any one of the projected signals. However, it has been observed that it may not yield physically meaningful IMFs, especially in cases where large number of projections are considered to compute the local mean.

#### IV. SIMULATIONS

We shall now illustrate the ability of QEMD to extract common modes present in multichannel data. For this pur-

---

#### Algorithm 2 Multivariate extension of EMD

---

- 1: Calculate a projection, denoted by  $p^{\theta_k}(t)$ , of the input signal  $q(t)$  along the direction vector  $\mathbf{x}^{\theta_k}$ , for all  $k$  (the whole set of direction vectors), giving  $\{p^{\theta_k}(t)\}_{k=1}^K$  as the set of projections;
- 2: Find the time instants  $\{t_i^{\theta_k}\}$  corresponding to the maxima of the set of projected signals  $p^{\theta_k}(t)$ ;
- 3: Interpolate  $[t_i^{\theta_k}, q(t_i^{\theta_k})]$  to obtain multivariate envelope curves  $\{e^{\theta_k}(t)\}_{k=1}^K$ ;
- 4: For a set of  $K$  direction vectors, the mean  $\mathbf{m}(t)$  of the envelope curves is calculated as:

$$\mathbf{m}(t) = \frac{1}{K} \sum_{k=1}^K e^{\theta_k}(t) \quad (8)$$

- 5: Extract the “detail”  $d(t)$  using  $d(t) = x(t) - m(t)$ . If the “detail”  $d(t)$  fulfills the stopping criterion for a quaternion IMF, apply the above procedure to  $x(t) - d(t)$ , otherwise apply it to  $d(t)$ .
-

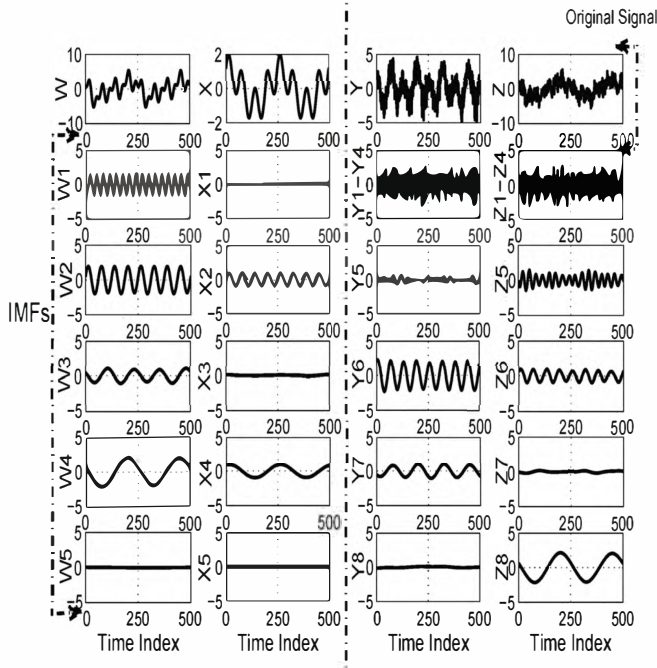


Fig. 3. Decomposition of two synthetic complex signals with components  $(W, X)$  and  $(Y, Z)$  obtained by two separate applications of the bivariate EMD algorithm. In general, the synchronization (mode alignment) among the four channels cannot be achieved as the input channels have been processed separately.

pose, we have conducted simulations on both synthetic data and on real world EEG signals. For both data sets, a set of  $K = 512$  direction vectors was used for taking signal projections.

#### A. Mode alignment using multivariate IMFs

The ability of the quadrivariate EMD algorithm to generate common scales embedded within the input quaternion signal is first demonstrated via simulations on a suitably designed synthetic signal; its four components (represented by  $W$ ,  $X$ ,  $Y$  and  $Z$ ) are shown in the top row of Figure 3. The data set was designed from four sinusoids such that one tone was present in all the components of the quadrivariate signal, whereas the remaining three tones were made common in  $WZ$ ,  $WY$  and  $WXZ$  components; two different realisations of white Gaussian noise were then added to the  $Y$  and  $Z$  channels. The resulting signal was then first processed by two separate applications of bivariate EMD algorithm [6], with  $WX$  and  $YZ$  acting as two separate complex inputs. In Figure 3, decompositions obtained from applying the bivariate EMD to the two input signals  $(W, X)$  and  $(Y, Z)$  are respectively shown in the left and right hand columns. It can be observed that different number of IMFs were obtained from the  $(W, X)$  and  $(Y, Z)$  components, making it difficult to synchronize the common oscillatory modes.

In the next step, all four channels were directly decomposed using the QEMD as shown in Figure 4. It can be seen in this case that the common modes (tones) are accurately aligned within the same quaternion IMFs; the

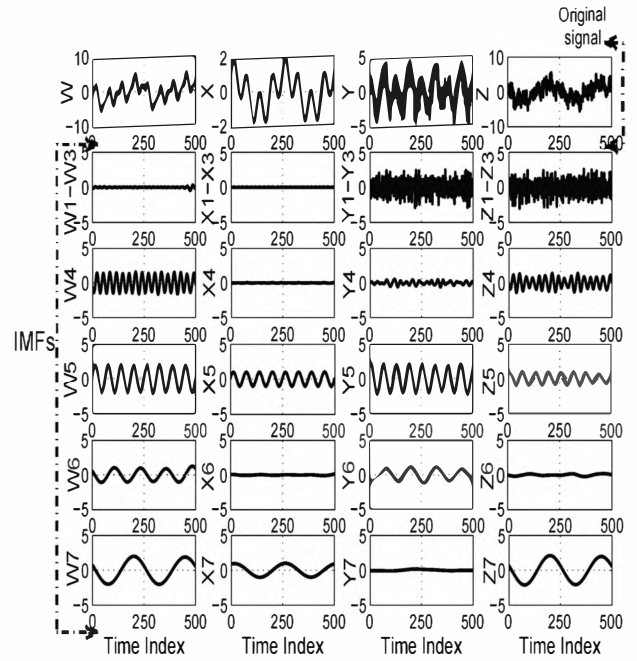


Fig. 4. Decomposition of a synthetic quaternion signal  $(W, X, Y, Z)$ , having multiple tones, obtained by the proposed QEMD algorithm. The synchronization among multiple channels of the input data has been achieved, as illustrated by the alignment of similar frequency tones within the same IMFs.

sinusoid common to all the components of the input was extracted in the IMFs  $W5$ ,  $X5$ ,  $Y5$ , and  $Z5$ ; whereas the remaining three tones were also accurately extracted in the respective IMFs. It is also worth noticing that, as designed, the high frequency Gaussian noise added originally in the  $Y$  and  $Z$  components was extracted in the respective channels of first three IMFs, while the  $W$  and  $X$  channels of the same IMFs carried practically no information. The synchronization, among multiple channels of the input signal, achieved in this manner makes QEMD a natural candidate for data fusion applications.

#### B. Denoising of real world EEG signals

We next applied the proposed method to the real world electroencephalography (EEG) signals with the aim to separate the brain electrical activity from unwanted artefacts such as the electrooculogram (EOG) and electromyogram (EMG). Solution to these problems is an important step for the accurate analysis of the information processing mechanism of the brain and is an active area of research [14]. Data used in these simulations were collected from 4 EEG channels ( $Fp1$ ,  $Fp2$ ,  $C3$ ,  $C4$ ), and subjects moved their eyes during the data collection resulting in ocular interference in recorded EEG signal.

The four channels ( $Fp1$ ,  $Fp2$ ,  $C3$ ,  $C4$ ) were then processed via QEMD. Owing to the mode alignment property of the proposed algorithm, the decomposed EEG data was synchronized in multiple quaternion IMFs in such a way that the high frequency neurophysiological signals were

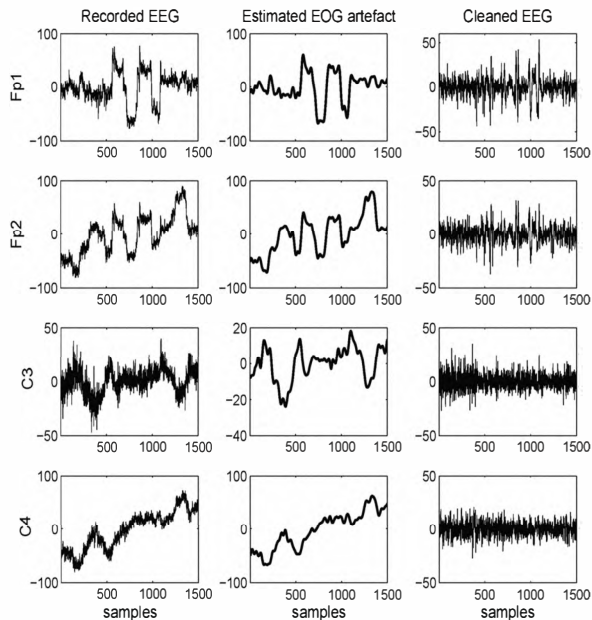


Fig. 5. Illustration of artefact removal from four EEG channels ( $Fp1$ ,  $Fp2$ ,  $C3$  and  $C4$ ) using quadrivariate EMD algorithm. The estimated muscle activity (artefact) has been shown in the middle column, whereas the denoised EEG signal is presented in the right column.

contained in the lower index IMFs, while low frequency electrophysiological signals (EMG and EOG) were present in the high index IMFs. Due to the mode alignment property of the proposed method, a simple threshold on the IMF index was used to separate non-EEG related interference from the underlying brain activity. The EOG and clean EEG signal estimated in this way are shown in the middle and right hand column of Figure 5, with the original contaminated EEG signals shown in the left hand column. It is important to note that such separation is difficult to achieve by applying univariate EMD on all the channels separately as this may result in spectrally uncorrelated components. For instance, in [14], a complex clustering technique is used in the frequency domain (Hilbert transform space) in order to identify spatially correlated modes from univariate EMD decompositions, however, to a certain extent, high frequency components were still present in the estimated EOG signal. There were no such problems noticed with QEMD as it effectively aligns the common modes present across multiple channels.

### C. Decomposition of RGB colored image

The ability of EMD to separate the natural frequency modes in a signal can also be used to decompose an image into its constituent 'subimages', where each 'subimage' corresponds to a separate frequency scale present in the original image [15] [16] [9]. We now illustrate the ability of our proposed QEMD method to decompose RGB based colored images into their constituent elements. This is possible due to the alignment of common frequency scales in Red, Green

and Blue decompositions obtained via QEMD.

To decompose the popular Lena image using QEMD, it was first represented in the RGB space. The three color channels (R, G and B) were then converted to vectors and combined to form a quadrivariate signal (the 4th component of the quadrivariate signal was made a zero vector) [17]. The resulting signal was then processed using the quadrivariate EMD. The IMFs obtained from this process were converted back to images and are shown in Figure 6, along with the original RGB image on the top left hand. It can be seen that the first few IMFs corresponding to the high frequency components carry the edge information within the signal; the low frequency components, such as the background colour, are extracted in the higher index IMFs.

## V. ACKNOWLEDGEMENTS

The data used in the EEG experiment was recorded in RIKEN Brain Science Institute, Japan. We also wish to thank Dr. T. M. Rutkowski for his help in the interpretation of the EEG results.

## VI. CONCLUSIONS

An extension of Empirical Mode Decomposition (EMD), termed the quadrivariate EMD (QEMD), has been proposed for the processing of quadrivariate signals. This is achieved by taking multiple real-valued projections of the input signal along multiple directions on a 3-sphere obtained by using the low discrepancy Hammersley sequence. The ability of the proposed method to extract common rotational modes across the signal components has been demonstrated via simulations on carefully designed synthetic data sets. The potential of the algorithm in the denoising of a real world nonlinear non-stationary EEG signal and in color image decomposition has also been demonstrated.

## REFERENCES

- [1] N. E. Huang, Z. Shen, S. Long, M. Wu, H. Shih, Q. Zheng, N. Yen, C. Tung, and H. Liu, "The empirical mode decomposition and Hilbert spectrum for non-linear and non-stationary time series analysis," *Proceedings of the Royal Society A*, vol. 454, pp. 903–995, 1998.
- [2] N. E. Huang and S. S. P. Shen, Eds., *Hilbert-Huang Transform and its Applications*, Singapore: World Scientific, 2005.
- [3] N. E. Huang and Z. Wu, "A review on Hilbert-Huang transform: Method and its applications to geophysical studies," *Reviews in Geophysics*, vol. 46, no. RG2006, 2008.
- [4] D. J. Duffy, "The application of Hilbert-Huang transforms to meteorological datasets," *Journal of Atmospheric and Oceanic Technology*, vol. 21, no. 4, pp. 599–611, 2004.
- [5] T. Tanaka and D. P. Mandic, "Complex empirical mode decomposition," *IEEE Signal Processing Letters*, vol. 14, no. 2, pp. 101–104, 2006.
- [6] G. Rilling, P. Flandrin, P. Goncalves, and J. M. Lilly, "Bivariate empirical mode decomposition," *IEEE Signal Processing Letters*, vol. 14, pp. 936–939, 2007.
- [7] M. U. Altaf, T. Gautama, T. Tanaka, and D. P. Mandic, "Rotation invariant complex empirical mode decomposition," in *Proceedings of the IEEE International Conference on Acoustics, Speech, Signal Processing*, 2007.
- [8] N. Rehman and D. P. Mandic, "Empirical mode decomposition for trivariate signals," *Accepted for IEEE Transactions in Signal Processing*, 2009.
- [9] D. Looney and D. P. Mandic, "Multi-scale image fusion using complex extensions of EMD," *IEEE Transactions in Signal Processing*, vol. 57, no. 4, pp. 1626–1630, 2009.

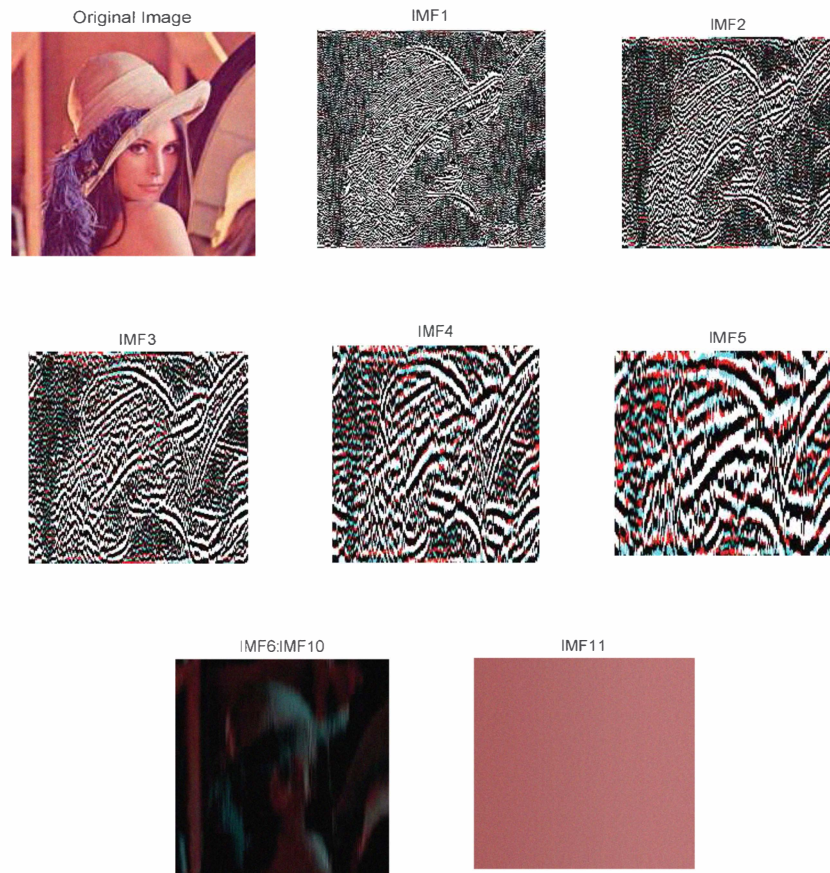


Fig. 6. Decomposition of the RGB Lena image using QEMD. The decomposed images corresponding to the lower index IMFs represent high frequency scales, e.g. edges (IMF1, IMF2), within the input image, whereas the higher index IMFs carry lower frequency scales such as the background color (IMF11).

- [10] N. Rehman and D. P. Mandic, "Multivariate empirical mode decomposition," *Proceedings of the Royal Society A (in print)*, 2010.
- [11] N. E. Huang, M. Wu, S. Long, S. Shen, W. Qu, P. Gloersen, and K. Fan, "A confidence limit for the empirical mode decomposition and Hilbert spectral analysis," *Proceedings of the Royal Society of London A*, vol. 459, pp. 2317–2345, 2003.
- [12] J. Cui and W. Freeden, "Equidistribution on the sphere," *Siam J. Sci. Comput.*, vol. 18, no. 2, pp. 595–609, 1997.
- [13] G. Rilling, P. Flandrin, and P. Goncalves, "On empirical mode decomposition and its algorithms," in *IEEE-EURASIP Workshop Nonlinear Signal Image Processing (NSIP)*, 2003.
- [14] T. M. Rutkowski, A. Cichocki, T. Tanaka, D. P. Mandic, J. Cao, and A. L. Ralescu, "Multichannel spectral pattern separation—an EEG processing application," *Proceedings of the IEEE International Conference on Acoustics, Speech, Signal Processing*, pp. 373–376, 2009.
- [15] A. Linderherd, "Compression by image empirical mode decomposition," *Proceedings of IEEE International Conference on Image Processing*, vol. 1, pp. 553–556, 2006.
- [16] H. Hariharan, A. Gribok, M. A. Abidi, and A. Koschan, "Image fusion and enhancement via empirical mode decomposition," *Journal of Pattern Recognition Research*, vol. 1, pp. 16–32, 2006.
- [17] N. L. Bihan and J. L. Sangwine, "Color image decomposition using quaternion singular value decomposition," *International conference on visual information engineering*, pp. 113–116, 2003.